

Reduced-Scale Experiments on the Water Suppression of a Rack-Storage Commodity Fire for Calibration of a CFD Fire Model

ANTHONY HAMINS and KEVIN MCGRATTAN
Building and Fire Research Laboratory
National Institute of Standards and Technology
Gaithersburg, MD 20899-8663, USA

ABSTRACT

The objective of this work was to provide measurements from reduced-scale experiments for use in the NIST Fire Dynamics Simulator, a computational fluid dynamics model that calculates fire growth, spread, sprinkler activation, and water suppression of rack-storage commodity fires. The model requires implementable sub-grid algorithms and corresponding data that adequately represent the full-scale heat and mass transfer that occurs in a warehouse fire with rack-storage of a standard commodity.

This paper describes experiments that investigated the effect of water application on the time to ignition and the heat release rate of the Group A Plastic Commodity. Several types of experiments were conducted including small-scale ignition measurements using the LIFT device and the cone calorimeter, and moderate-scale heat release rate measurements using oxygen consumption calorimetry. Both ignition and heat release rate measurements were made with and without water application. The results showed that the heat release rate is adequately described as a function of the water application rate in a form suitable for implementation in a CFD fire model.

KEY WORDS: CFD fire models, rack storage fire, water sprinklers, fire suppression

INTRODUCTION

A challenge facing computational fluid dynamics (CFD) fire models involves adequately representing fire phenomena in a way that preserves the underlying physics and is at the same time tractable computationally. The objective of this work was to provide measurements from appropriate reduced-scale experiments to be used as input data for the NIST Fire Dynamics Simulator (FDS), a CFD model that calculates and visualizes fire spread, growth, and sprinkler suppression in a large enclosure. FDS solves numerically the conservation equations of mass, momentum and energy that govern low-speed, thermally-driven flows with an emphasis on heat transfer associated with fire. This work focuses on application of the model to simulate the burning and suppression of a rack-storage commodity fire, a topic that has been the focus of previous research [1-3].

A CFD model requires information applicable to the spatial resolution of the model, which is limited by the size of the domain and the calculation time. In models of the full-scale problem, the domain is 50 m by 50 m by 20 m and a single cell of the

computational grid in this study is typically 10 cm to 20 cm. Phenomena that occur at smaller scales cannot be modeled directly, but must be described through sub-models and empirical correlations. The FDS model requires information on the flammability properties of the fuel, including the ignition and the local heat release rate, both with and without water application. A detailed discussion of FDS is found in McGrattan et al. [4,5]. Details regarding the FDS computational scheme as applied to the rack-storage problem can be found in the companion reports [6,7].

The fuel selected for consideration in this study was the FM Standard Plastic Commodity also known as the Group A Plastic Commodity*, which is commonly used by fire testing laboratories to test the effectiveness of water sprinklers and other fire protection devices [8]. The Group A Commodity is a multi-component fuel composed of compartmentalized unexpanded polystyrene cups within corrugated paper cartons. Eight cartons loaded on a wood pallet comprise one pallet-load of the Commodity. Each carton is 0.53 m wide, 0.53 m deep, and 0.50 m high. Vertical and horizontal cardboard dividers form 125 cells in a 5 x 5 x 5 array. Within each cell is one polystyrene cup, which weighs 36 g and has a 0.45 L capacity. The mass of the constituents of one (conditioned) box procured from UL is shown in Table 1 including the combined standard uncertainty, which is dominated by instrument reading accuracy. The mass of the constituents of the Group A Commodity reported by Yu et al. [1] differs by as much as 20 %. Although the mass of plastic cups is twice that of the cardboard, the early fire behavior is dominated by the burning of the corrugated paper.

Yu et al. [1] performed a series of large-scale fire suppression tests for two standard commodities. The results were analyzed in terms of a global heat balance model, which assumed a form for the total fire heat release rate after water application, $\dot{Q}(t)$, as:

$$\dot{Q}(t) = \dot{Q}_o \cdot \exp[-k(t-t_o)] \quad (1)$$

where \dot{Q}_o is the total heat release rate at the time of water application (t_o), and k is an

Component	Mass (kg)	Mass Percent	H_c/r_o^A (MJ/kg of O ₂)
Corrugated Paper	2.5±0.1	36±1	13.19 ^B
Polystyrene Cups	4.5±0.01	64±1	13.61
Average per box	7.0±0.1	100	13.46±0.13
A. Ref. 9			
B. Data for cellulose [9]			

* Certain trade names and company products are mentioned in the text to specify adequately the experimental procedure and equipment used. In no case does such identification imply recommendation or endorsement by NIST, nor does it imply that the products are necessarily the best available for the purpose.

empirical parameter related to the suppression, which accounts for the fuel density, fuel specific heat, ignition temperature, heat of combustion, total burning rate, heat of pyrolysis, and average water application rate. Yu et al. [1] showed that the coefficient k can be correlated as a linear function of the water application rate for the period 240 s after the time of water application. The value of k was different for the two types of commodities tested. Yu's model cannot be directly applied in a CFD calculation because it is a global suppression model. Although it predicts the effect of water application on the total heat release rate, it does not predict the local heat release rate associated with a small section of the burning commodity. FDS requires flammability information based on the local fuel behavior including its ignition character and heat release rate. FDS models fire spread by tracking heat transfer from the fire to the fuel [4,5]. Sprinkler activation is predicted and droplet trajectory is tracked. Vitiation is neglected because water effects are thought to dominate suppression in the rack-storage problem.

Although Yu's model (Eq. 1) is not directly applicable to the FDS methodology, an analogous functional form was sought that relates the local heat release rate to the local water application rate. This information could not be extracted from experiments using a cone or a small-scale calorimeter, as such experiments do not adequately replicate the local thermal environment experienced by a single cell within the full-scale burning commodity [10]. For this reason, moderate-scale experiments were conducted.

Two types of experiments were conducted in this study. The first measured the time required for ignition of the corrugated paper with and without water application as a function of the incident heat flux. The second series of experiments measured the effect of water application on the heat release rate of the burning commodity. Discussion of other reduced-scale experiments conducted to develop input (such as the fuel radiative heat loss fraction) for the NIST Fire Dynamics Simulator (FDS) can be found in Hamins and McGrattan [10].

EXPERIMENTAL APPARATUS and PROCEDURE

This section describes the experimental apparatus and the procedures used to characterize the ignition and the heat release rate of the Plastic A Commodity.

Ignition

The time to sustained flaming was measured using a sample of the outer shell of the commodity oriented in a vertical configuration in the LIFT apparatus. The LIFT has been described in detail previously [11]. Some experiments were conducted using the cone calorimeter [12] and the prescribed standard test protocols. As in all experiments, the samples were conditioned at standard conditions (50% relative humidity and a temperature of 20° C) before tests. The incident heat flux on the sample surface was measured using a calibrated total heat flux gauge. The sample was placed in front of the radiant source, covered by a thick marine board. The board was removed and the time to sustained flaming was measured using a stopwatch. For all experiments, the direction of the ribs or flues of the corrugated paper was maintained vertically.

The time to sustained flaming due to application of water on the exposed surface of a horizontally oriented corrugated paper sample was investigated using the cone calorimeter [12]. The sample was positioned horizontally to promote uniform water evaporation and a uniform heat flux on the sample surface. The experiments were performed only in the cone calorimeter, because the LIFT device requires vertical orientation of the sample.

The sample was weighed before water application. Water was applied with a small brush and allowed to soak into the sample for approximately two minutes. The mass of the sample was measured just before testing to avoid significant water evaporation. The sample was covered until the experiments were initiated.

Heat Release Rate as a function of Water Application

The experiments were performed at Underwriters Laboratories. In total, 19 experiments were conducted. The entire fuel/nozzle arrangement was located below a large exhaust hood that was instrumented to measure the heat release rate using oxygen consumption calorimetry in accordance with ASTM E1590-01 [13]. The measurement was calibrated using propane fires with a heat release rate similar to that in the experiments. The fuel

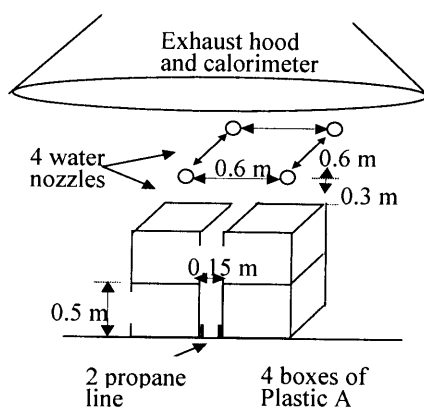


Fig. 1 Fuel and nozzle arrangement for Tests 1-19.

arrangement shown in Fig. 1 consisted of four boxes of the Plastic A commodity stacked two high, like a standard pallet. The two stacks were positioned 15 cm from each other, creating a flue that had the same separation as that used in full-scale testing. A pair of propane line igniters was positioned across the entire flue, at the base of the boxes. The water applicator was supported such that its four identical water nozzles were positioned symmetrically about the center of the flue and 30 cm above the box tops. The nozzles were arranged on the corners of a square with 0.6 m sides, providing water coverage over a 1.49 m² area. Pan measurements demonstrated that the applied density was approximately uniform.

In the experiments, the water nozzles were positioned close to the commodity, not unlike the FM Required Delivered Density (RDD) tests [1]. It is thereby assumed that the plume had little effect on the droplet trajectory. The nozzles were not directly above the flue space, so only a small number of droplets penetrated the upper portions of the flue space. The nozzles were connected to a 8 cm diameter water line that was wrapped by approximately 1 cm of ceramic fiber insulation to avoid heating. Several nozzle sizes were used, depending on the desired water flux. Table 2 lists the average water application flux (\dot{M}_{wf}'') and the time of water application. The water application time was varied from 30 s to 200 s and the water flux was varied from 0.03 kg/m²-s to 0.66 kg/m²-s. These values covered the full range of interest. For example, Yu et al. [1] found that water suppression was achieved with an average flux of 0.08 kg/m²-s in a two tier fire.

Table 2. Time & Rate of Water Application during the HRR Experiments.			
Experiment No.	Application Time (s)	Avg. Water Flux \dot{M}_{wf}'' (kg/m ² -s)	Water Application per Surface Area M_w'' (kg/m ²)
1	380	0.66	0.16
2	470	0.38	0.092
3	65	0.28	0.067
4	106	0.28	0.067
5	115	0.074	0.018
6	122	0.074	0.018
7	150	0.053	0.013
8	93	0.074	0.018
9	93	0.14	0.034
10	110	0.14	0.034
11	205	0.14	0.034
12	116	0.11	0.026
13	63	0.11	0.026
14	64	0.19	0.046
15	71	0.053	0.13
16	62	0.032	0.0077
17	104	0.032	0.0077
18	58	0.053	0.013
19	30	0.053	0.013

The propane line igniters were composed of two parallel 30 cm long and 12.5 mm diameter copper tubes. Along the top of each tube, 1 mm diameter holes were drilled every 1 cm. The tubes were separated by a 12.5 cm gap. The propane flow through the igniter was approximately 0.5 L/s, yielding a 40 kW fire that was nearly 50 cm in height. The igniter was allowed to burn for 30 s. The igniter flames entirely covered the vertical sides of the boxes in the flue space. Table 1 shows that the ratio of the heat of combustion per mass of oxygen consumed (H_c/r_o) for the constituents of the Plastic A commodity are similar (within 4). A mass weighted average H_c/r_o was used in the heat release rate determination from the oxygen consumption calorimetry measurements.

RESULTS and DISCUSSION

Ignition

As the conditioned corrugated paper sample was exposed to the incident flux, a black char layer formed on its surface. Figure 2 shows results from the LIFT experiments for the time to flaming ignition as a function of the incident heat flux (\dot{q}_{ext}''). The time to ignition increased as the incident flux decreased until a critical flux was obtained below which sustained flaming was not obtained. For flux levels less than 14 kW/m², the sample smoldered, but flaming ignition did not occur before the entire sample smoldered away. For flux levels less than 20 kW/m², the sample first smoldered and only later was a sustained flame observed. Use of the LIFT is preferred over the cone for low fluxes,

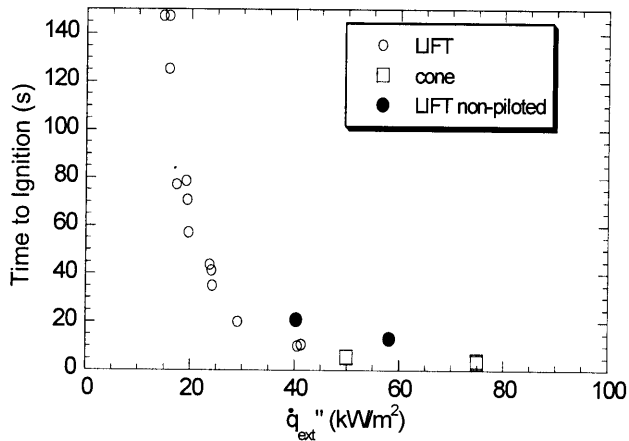


Fig. 2 The time to flaming ignition of a conditioned sample of corrugated paper as a function of the incident flux, \dot{q}''_{ext} .

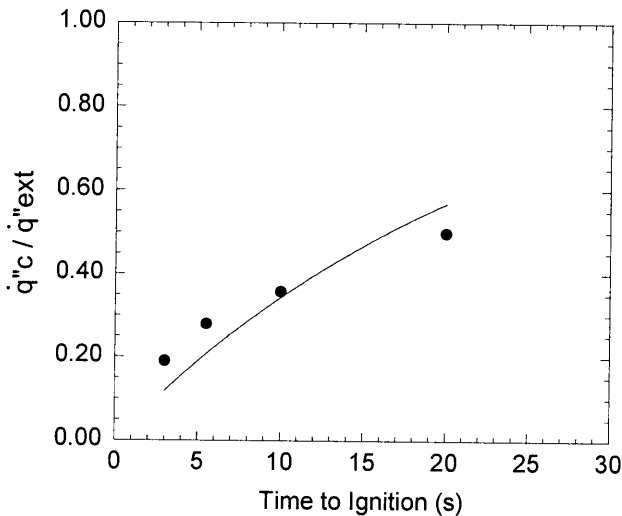


Fig. 3 The ratio of the critical to the external flux as a function of time to ignition.

Such a plot allows interpretation of a sample's flammability in terms of a thermally thin analysis [14]. A fit to the data in the form shown in Fig. 3 yields an exponential term whose coefficient is equal to the ratio of an effective heat transfer coefficient, h , to the lumped thermal parameter, $c_p \rho \delta$, which is the product of the effective specific heat, density, and thickness of the material. The ignition temperature and the value of h were estimated as 370°C and $0.042 \text{ kW/m}^2\text{K}$, respectively, based on the thermally thin analysis. Treatment of the corrugated paper as thermally thick would also be a reasonable method, but for reasons of computational efficiency, the thermally-thin approach was used here.

because the sample size is significantly larger, which affects the probability of flaming ignition. Because flux levels in the LIFT device are limited, the cone calorimeter was used for moderate to high flux levels ($>40 \text{ kW/m}^2$). A very large number of flaming brands were observed during the full-scale experiments suggesting that piloted ignition is representative of the warehouse fire problem. It is also possible that non-piloted ignition could occur during the phenomena of aisle jumping. To study the effect of the pilot flame on ignition, a number of non-piloted ignition experiments were conducted. Figure 2 shows that non-piloted ignition required significantly longer preheat times than piloted ignition. The critical ignition flux (\dot{q}''_c) is found by fitting a straight line in a plot of the reciprocal of the time to ignition as a function of the applied external flux for the data in Fig. 2 and noting at what flux the time to ignition becomes infinite [14]. The critical flux was approximately ratio of flux is plotted as a function of the time to ignition.

Total heat flux measurements conducted at UL on moderate-scale fire tests involving two to four layers of pallets in a rack storage configuration indicate that a heat flux of 90 kW/m^2 to 110 kW/m^2 impinges on the surface of the boxes when flames are present in the vertical flue space. When flames are not present in the flue space, the heat flux on the box surfaces is relatively small. Therefore, in Fig. 3, only data for fluxes greater than 30 kW/m^2 were used to determine $c_p \rho \delta$, leading to a value of $0.98 \text{ kJ/m}^2\text{-K}$. The high flux data in Fig. 3 appear to be adequately fit using this approach.

Effect of Water on Ignition

Figure 4 shows the results from experiments testing the effect of water application in delaying the time to flaming ignition of the corrugated paper sample. The figure presents the ignition time as a function of the mass of water applied per unit area of cardboard for an incident flux of 20 kW/m^2 and 25 kW/m^2 . Idealized behavior in the figure is indicated by the solid lines and was based on the assumptions that (1) the incident heat flux, water application, and evaporation were uniform over the sample surface and that (2) the

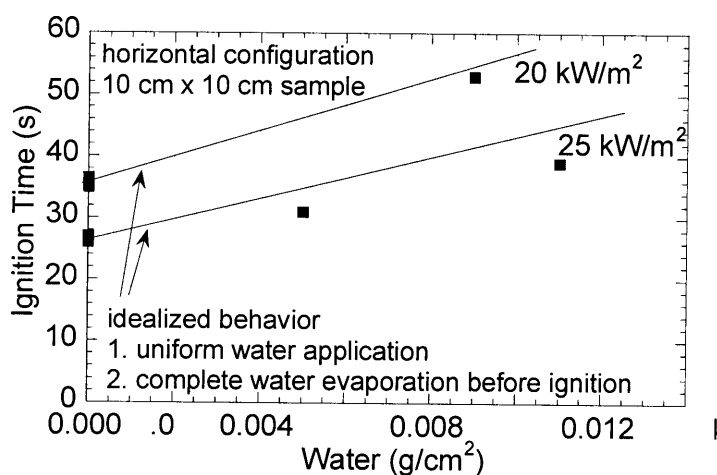


Fig. 4 The ignition time as a function of water applied per unit area.

applied water was completely evaporated before ignition. Fig. 4 shows that the measured time to ignition appears to be adequately represented by the idealized behavior. In summary, application of water on an intact portion of the commodity can significantly delay or prevent ignition, depending on the incident heat flux and the water application flux.

Heat Release Rate

The heat release rate (HRR) results for Tests 1-19 were very similar for all tests for the first 30 s of burning. The corrugated paper rapidly ignited ($\sim 5 \text{ s}$) and the flames quickly grew, reaching nearly 1.5 m just 10 s after ignition. The flames shortened 20 s after ignition and the HRR decreased as the outermost cardboard sheet burned away and the polystyrene cups began to melt (see HRR in Fig. 5). Video record of the experiments showed that the boxes burned in a nearly uniform manner from the flue in, along the entire surface of the box. Thus, the dominant contributor to the HRR appeared to be from burning in the flue, although flames were also observed on the box tops, more so at later times in the experiments. After several minutes, the boxes collapsed into a burning pile. The measurements were continued, providing useful data on the effect of water application on the HRR. Similar behavior was observed in full-scale.

At the time of water application, there was an initial rapid decrease in the heat release rate. Depending on the application rate, the HRR often increased slowly with time. This behavior occurred in Tests 8, 9, 10, and 16, and more prominently in Tests 13-15 and 17-19. In these experiments, either small water fluxes were applied or the application times were relatively late in the experiment. The HRR measurements were well-fit by the following functional form:

$$\dot{q}''(t) = \dot{q}_o''(t) \cdot [(\exp(k_1[t-t_0])) + k_2[t-t_0]] \quad (2)$$

where $\dot{q}''(t)$ is the local heat release rate per unit area, $\dot{q}_o''(t)$ is the heat release rate per unit area without water application, and k_1 and k_2 are the local suppression coefficients (s^{-1}), which are equal to zero for $t < t_0$. As in Eq. 1, t_0 is the time of water application. The form of Eq. 2 is similar to Yu's correlation (Eq. 1) except that there is an additional term

involving k_2 , which represents the observation that $\dot{q}''(t)$ slowly increases with time after an initial rapid decrease in the heat release rate. The HRR results from Tests 1 and 2 are shown in Fig. 5. In these experiments, the water was not applied until very late (> 400 s). The data from Tests 1 and 2 were averaged and smoothed to determine a representative profile of $\dot{q}_o''(t)$, which is the basis for understanding the effect of the applied water flux.

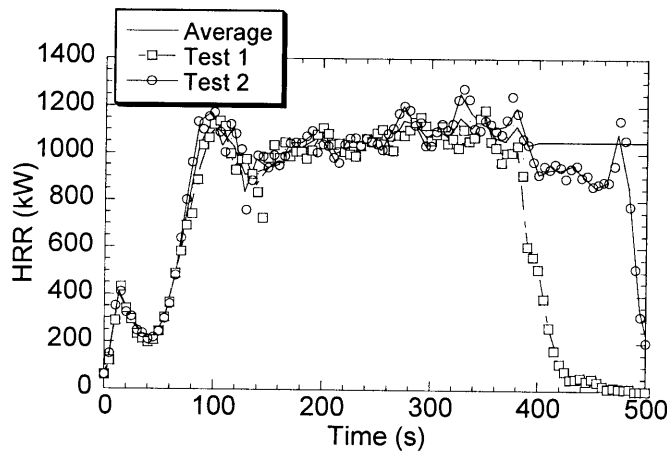


Fig. 5 The measured heat release rate without water application measured in Tests 1 and 2.

Following Yu et al., k_1 is taken as proportional to the water application rate:

$$k_1 = a_1 M_w'' \quad (3)$$

where a_1 is a constant ($m^2/kg \cdot s$) and M_w'' is the average water application mass per unit exposed area of the commodity surface (kg/m^2). M_w'' is defined as:

$$M_w'' = \dot{M}_{wf}'' \cdot A / (U \cdot P) \quad (4)$$

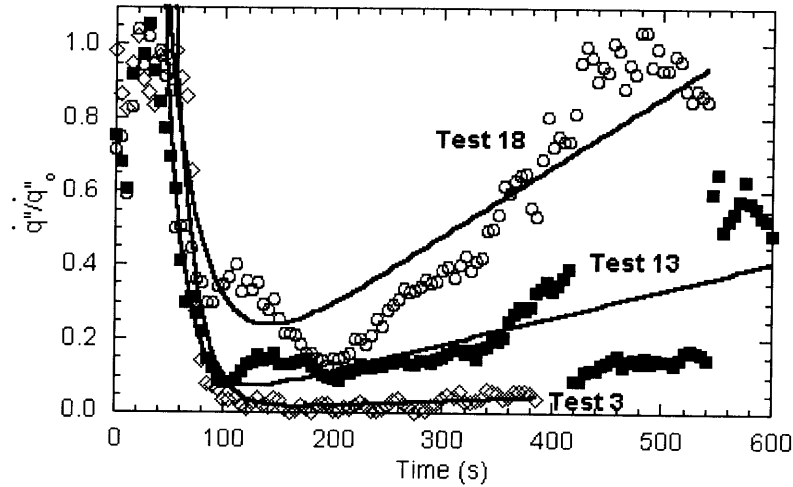


Fig. 6 The normalized heat release rate measurements (\dot{q}'' / \dot{q}''_o) and fits using Eq. 2 for Tests 3, 13, and 18.

where \dot{M}''_{wf} is the average water flux at the top of the boxes ($\text{kg}/\text{m}^2\text{-s}$), A is the surface area of a single box top (0.28 m^2), U is a reference speed (0.54 m/s) taken as the water cascade speed [15], and P is the perimeter along the top of a single box unit (2.12 m). Thus, $M''_w = (0.24 \text{ s}) \dot{M}''_{wf}$. Use of the parameter M''_w comes out of the development of the FDS code [15]. The values of \dot{M}''_{wf} and M''_w are listed in Table 2. When $M''_w = 0$, $\dot{q}'' = \dot{q}''_o$. Figure 6 shows the normalized HRR measurements and fits (\dot{q}'' / \dot{q}''_o) for three of the experiments, which were selected for presentation because they represent similar water application times, but very different application rates (see Table 2). The fits appear to adequately represent the data, demonstrating that the form of Eq. 2 is suitable for a broad range of water application rates - from fires that are suppressed (Test 3) to

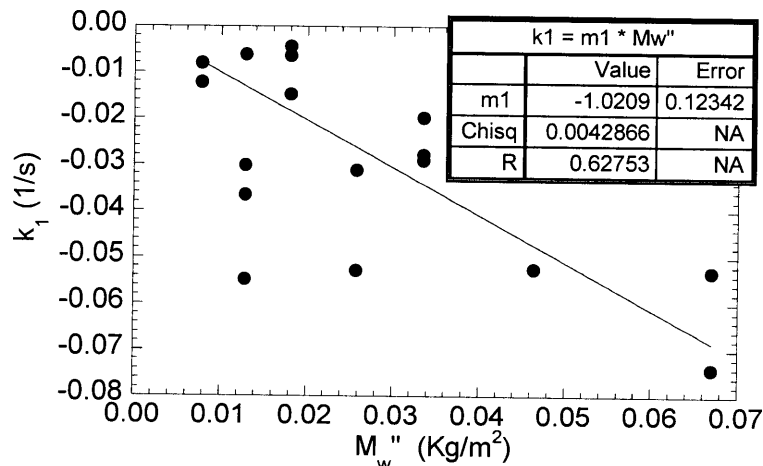


Fig. 7 The value of k_1 as a function of the water application rate (M''_w) for Tests 3-19.

those that experience a rate of water application inadequate to achieve suppression (Tests 13 and 18). The other HRR measurements were also well-fit by Eq. 2 [10].

Figure 7 shows the value of k_1 as a function of the water application rate (M_w''). From the figure, the best-fit value for a_1 (Eq. 3) is equal to -1.0. The value of a_1 is negative, because water application decreases the heat release rate. The value of k_2 (s^{-1}) was also related to the water application rate. Figure 8 shows k_2 as a function of the water mass per unit area for all of the experiments listed in Table 2. A straight line fit to the data yields:

$$k_2 = a_2 M_w'' + b_2 \quad (5)$$

and the values of a_2 and b_2 are equal to $-0.020 \text{ m}^2/\text{kg}\cdot\text{s}$ and 0.0015 s^{-1} , respectively, as determined by the best-fit line shown in Fig. 8. When $t < t_0$, then the values of the constants k_2 , a_2 , and b_2 are defined as zero, insuring that \dot{q}'' is equal to \dot{q}_o'' in Eq. 11. The fits for k_1 and k_2 yield values that are related to both the water application rate and the time of water application, reflecting the observation that water application is less effective at late application times.

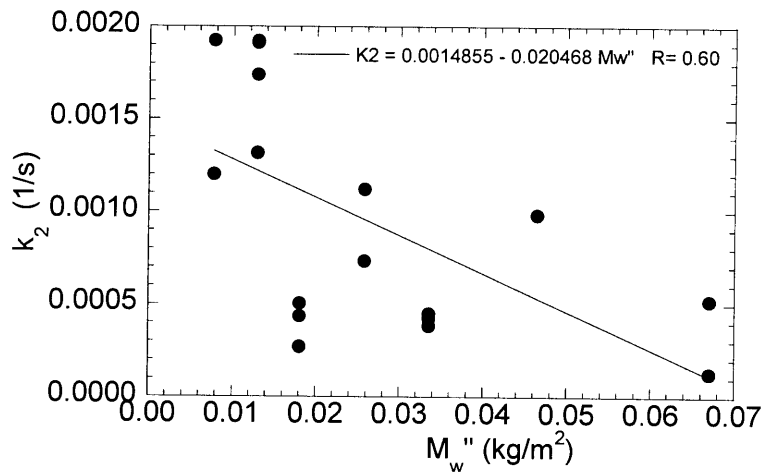


Fig. 8 The value of k_2 as a function of the water application rate (M_w'') for Tests 3-19.

SUMMARY

This paper highlights the input needs of a CFD fire model. A series of experiments was conducted to characterize the flammability of the Group A Plastic Commodity undergoing water suppression in a rack-storage configuration. Although the fuel is arranged in a simple rack-storage array, the burning process is complex due to the nature of the multi-component nature of the fuel, which is composed of compartmentalized plastic cups and corrugated paper.

The results showed that the heat release rate is adequately described as a function of the water application rate in a form suitable for implementation in a CFD fire model. The most important parameter is k_1 , the coefficient of the exponential term, which describes the effect of water application on the heat release rate. A second parameter, k_2 , the coefficient of the linear growth term, describes the rather slow continued burning of this complex multi-component fuel at times long after water has been applied.

Although the scatter in the values of k_1 and k_2 appear to be large, the efficacy of the approach and associated input data should be judged in terms of the predictive capability of the model, which has proved to be able to differentiate between those experiments that activated a large number of sprinklers and those that activated a small number [McGrattan et al., 1999]. The model also provides valuable insight into what occurred in the experiments and also what would have occurred in the event of changes in test parameters. In principle, the methodology developed here could be used on any of the standard rack-storage commodities. The cost of the research associated with gathering input for even a single fuel type, however, is quite high, even though the application was a rather simple geometric configuration within a well-defined fire scenario.

ACKNOWLEDGEMENTS

The authors are grateful to Dr. Jukka Hietaniemi of VTT Building Technology (Finland), Dave Sheppard of ATF, Steve DiGiovanni, and Roy McLane (NIST) for helpful discussions and assistance with the measurements.

REFERENCES

1. Yu, H-Z, Lee, J.L., Kung, H-C., *Proc. 4th Int. Sym. on Fire Safety Science*, 901-912, 1994.
2. Chan, T-S, Kung, H-C, Yu, H-Z, and Brown, W., *Proc. 4th Int. Sym. on Fire Safety Science*, 913-924, 1994.
3. Lee, J.L., *Proc. 1st Int. Sym. on Fire Safety Science*, 1177-1186, 1986.
4. McGrattan, K., Baum, H.R., Rehm, R.G., *Fire Safety Journal*, 30, 161-178 (1998).
5. McGrattan, K., Hamins, A., Stroup, D., *Sprinkler, Smoke, Heat Vent, Draft Curtain Interaction – Large Scale Experiments and Model Development*, NIST Technical Report NISTIR 6196-1, NIST, Gaithersburg, MD, 1998.
6. McGrattan, K., Baum, H.R., Rehm, R.G., Hamins, A., and Forney, G.P., *Fire Dynamics Simulator-Technical Reference Manual*, NIST Internal Report NISTIR 6467, National Institute of Standards and Technology, Gaithersburg, MD, January 2000.

7. McGrattan, K., and Forney, G.P., *Fire Dynamics Simulator-User's Manual*, NIST Internal Report NISTIR 6469, National Institute of Standards and Technology, Gaithersburg, MD, January 2000.
8. Sheppard, D.T., *Heptane Burner Tests and Commodity Tests*, International Fire Sprinkler, Heat & Smoke Vent, Draft Curtain, Fire Test Project, National Fire Protection Research Foundation (NFPRF) Technical Report, Batterymarch Park, Quincy, MA, April 1998.
9. Babrauskas, V., *Appendix A*, Fire Protection Handbook (Ed.: A. Cote), 18th edition, National Fire Protection Association, Quincy MA, 1997.
10. Hamins, A., and McGrattan, K., *Reduced-Scale Experiments to Characterize the Suppression of Rack-Storage Commodity Fires*, NIST Internal Report NISTIR 6439, NIST, Gaithersburg, MD, November 1999.
11. ASTM E-1321-90, *Standard Test Method for Determining Material Ignition and Flame Spread Properties*, American Society for Testing and Materials, Philadelphia, PA, 1990.
12. ASTM E-1354-94, *Standard Test Method for Heat and Visible Smoke Release for Materials and Products Using an Oxygen Consumption Calorimeter*, American Society for Testing and Materials, Philadelphia, PA, 1994.
13. ASTM E1590-01, *Standard Test Method for Fire Testing of Mattresses*, American Society for Testing and Materials, West Conshohocken, PA, 2001.
14. Ohlemiller, T.J., and Villa, K.M., *Material Flammability Test Assessment for the Space Station Freedom*, Technical Report NISTIR 4591, National Institute of Standards and Technology, Gaithersburg, MD 20899, 1991.
15. McGrattan, K.B., Hamins, A., Forney, G.P., *Proc. 6th Int. Sym. on Fire Safety Science*, 505-516, 1999.